Fiber-coupled ultrashort-pulse-laser-based electronic-excitation tagging velocimetry

PAUL S. HSU, [1,*] NAIBO JIANG,[1] PAUL M. DANEHY,[2] JAMES R. GORD,[3] SUKESH ROY[1]

[1]Spectral Energies LLC, Dayton, OH 45431, USA
[2]Advanced Measurements and Data Systems Branch, NASA Langley Research Center, Hampton, VA 23681, USA
[3]Air Force Research Laboratory, Aerospace Systems Directorate, Wright-Patterson AFB, OH 45433, USA
*Corresponding author: paul.hsu@spectralenergies.com

Transmission of intense ultrashort laser pulses through hollow-core fibers (HCFs) is investigated for molecular-tagging velocimetry. A low-vacuumed HCF beam-delivery system is developed to transmit high-peak-power pulses. Vacuum pressure effects on transmission efficiency and nonlinear effects at the fiber output are studied for 100-ps and 100-fs laser beams. With a 0.1 bar vacuum in the fiber, transmission efficiency increases by ~30%, while spectral broadening is reduced. A 1-m-long, 1-mm-core metal-dielectric-coated HCF can transmit ~45 mJ/pulse and ~2.9 mJ/pulse for 100-ps laser pulses (at 532 nm) and 100-fs laser pulses (at 810 nm), respectively. Proof-of-principle, single-laser-shot, fiber-coupled, ps- and fs-laser-based, nitrogen electronic-excitation tagging velocimetry is demonstrated in a free jet. Flow velocities are measured at 200 kHz to capture high-frequency flow events.

1. INTRODUCTION

Flow-velocity measurements in high-speed turbulent flows are essential for the fundamental understanding and optimization of air vehicles, space vehicles, and modern gas-turbine engines. Several optical techniques have been widely used for velocimetry, including Particle-Image Velocimetry (PIV) [1,2], Molecular-Tagging Velocimetry (MTV) [3–5], Planar Doppler Velocimetry (PDV) [6,7], and Laser Doppler Velocimetry (LDV) [8]. These techniques require the addition of seed particles or molecules to the flow for tracking. By measuring the displacements of the seed particles within a certain time delay, the one-dimensional (1-D) or two-dimensional (2-D) velocity field can be determined. However, the addition of seed particles or molecules may not be practical for a wide range of transonic, supersonic, and hypersonic flow facilities. For example, seeding can alter the mean flow and introduce unsteady disturbances [9,10]. Moreover, the seeded tracers can contaminate the ground-test facility, which increases the maintenance cost and decreases the effective run time, particularly in large-scale wind tunnels.

Several non-seeded laser-based molecular velocimetry techniques such as Raman excitation plus laser-induced electronic fluorescence (RELIEF)[11–13], filtered Rayleigh scattering (FRS) [14], interferometric Rayleigh scattering (IRS) [15,16], laser-induced thermal acoustics (LITA) [17] and air photolysis and recombination tracking (APART) [18] have been implemented for gas flow velocity measurements. All the approaches mentioned above have their own advantages and limitations in terms of dynamics range, spatial resolution, and complexity. For example, RELIEF technique can be used for air flows, but it requires three laser beams with different wavelengths which increases experimental complexity. Recently, non-seeded velocimetry using ultrashort-pulse-laser electronic-excitation MTV with ps [19] and fs [20–23] laser pulses is developed. This technique is a seedless nitrogen-fluorescence-based velocimetry technique; it is suitable for point or 1-D velocity measurements in subsonic and supersonic flows. This method requires only a focused ultrashort-pulse-laser beam and an intensified camera. N_2 molecules are photodissociated by an intense laser pulse to form significant populations of $N(^4S)$ atoms [20], which undergo three-body recombination to form metastable, electronically excited nitrogen N_2 ($^5\Sigma_g^+$) and, subsequently, a vibrationally excited nitrogen B state ($v'\approx11$). The fluorescence emission from the long-lifetime B state of N_2 ($B^3\Pi_g \rightarrow A^3\Sigma_u^+$) can continue for a relatively long period of time (~20 μs), enabling velocity measurement by tracking the fluorescent N_2 molecules. A high-intensity, ultrashort laser pulse is preferred for this technique because of its low laser-heating effect on the measured flow fields [11,12,15]. In general, the use of a fs- and ps- duration laser for electronic-excitation tagging is called FLEET and PLEET, respectively. FLEET was first demonstrated by Michael et al. in 2011 [20] and PLEET by Jiang et al. in 2017 [19]. The major advantages of these methods for measurements in practical wind tunnels are: 1) relatively straightforward experimental setup aided by a single-laser-beam and a single-camera, 2) no need to seed the flow either with particles or other molecules, and 3) the technique is based on nitrogen fluorescence (nitrogen being the most commonly used and abundant gas in large ground-test facilities which typically operate on air or nitrogen). When PLEET and FLEET diagnostics are implemented in harsh and physically restricted environments, traditional experimental approaches that are based on free-standing optics face stiff challenges because of vibrations, unconditioned temperature (both hot and cold),

velocity and humidity, large thermal gradients, and limited or no optical access. These difficulties can be overcome by transmitting the required laser beams through optical fibers to the probe region, with the laser system and detection hardware being located remotely in a climate-controlled facility. Fiber-coupled PLEET and FLEET systems would: 1) reduce the need for free-standing optics in test-cell environments; 2) provide flexibility with the ability to access non-windowed test sections when needed; 3) isolate the high-power laser system from heat or cold and vibration; and 4) provide safe, guided, and confined laser-beam delivery.

The PLEET and FLEET techniques require high-peak laser intensity at the probe volume to enable efficient dissociation of the N_2 molecule through multiphoton excitation process. Typically, the amount of energies needed for a 100-ps-duration pulse and a 100-fs-duration pulse are ~10 mJ/pulse [19] and ~1 mJ/pulse [20–23], respectively. Such high-energy requirements impose significant constraints on fiber-coupled PLEET and FLEET because of the intrinsic optical-damage threshold of the fibers. The enhanced, higher-order nonlinear processes during propagation of intense laser beams through the fiber can also cause spectral and temporal broadening of the input laser beam and, hence, reduce the efficiency of the multiphoton excitation [24].

Ideally, a fiber-coupled ultrashort-pulse laser beam delivery system for PLEET and FLEET velocimetry requires sufficient energy/intensity that a fluorescence signal with reasonable signal-to-noise ratio (SNR) can be generated. The amount of laser energy/intensity that can be delivered in such a system is limited by the damage threshold of the fiber for varying pulse durations, the physical structure of the fiber, and the wavelength of the input laser beam. Previous fiber studies have shown inability of the solid-core fiber to transmit the required ps laser pulse because of the relatively low damage threshold (maximum transmission of 150-ps pulse through a 1-mm-core silica fiber is ~3.3 mJ/pulse [25]). Another drawback of the solid-core fiber for laser-beam delivery is spectral and temporal broadening of the pulse because of the broadband material dispersion, particularly for fs-pulse delivery [25]. Typically, solid-core-silica-fiber damage tends to occur in the core at high input power, causing impairment either at the entrance surface or within the fiber because of self-focusing effects [24–27]. Hollow-core fibers are of interest because in absence of a solid core all the above problems can be avoided [28–32]. Recently, Jelinkova et al. [30] and Li et al. [32] demonstrated that hollow-core capillary fibers can transmit high-power laser beams with 50-ps-duration laser pulses (~40 mJ/pulse at 1046 ns) and with 100-fs-duration laser pulses (~1.4 mJ/pulse at 800 nm).

The objective of this study is to investigate the feasibility of delivering intense ps and fs laser pulses through a commercially available hollow-core capillary fiber and investigate fiber-based PLEET and FLEET velocimetry in high-speed nitrogen flows. Optical-damage threshold, output-beam quality, nonlinearities inside the fiber, and temporal distortion of the input laser pulses are studied. Proof-of-principle, single-laser-shot, fiber-coupled, PLEET and FLEET velocimetry in a nitrogen jet are demonstrated.

The outline of this paper is as follows. The experimental arrangement used for fiber-coupled PLEET and FLEET is described in Section 2. In Section 3, the fiber-transmission characteristics are presented. Section 4 contains a demonstration of fiber-coupled PLEET and FLEET. A summary is presented in Section 5.

2. EXPERIMENTAL SETUP

A schematic diagram of the optical system for coupling high-power, ultrashort laser pulse through the hollow-core fiber is shown in Fig 1. Ti:Sapphire laser (Elite Duo, Coherent) that produces ~5 mJ/pulse at 1-kHz pulse repetition rate with pulse duration 100 fs at 810 nm is used as a fs source. The ps laser is a 10-Hz Nd:YAG Regenerative Amplifier system, which generates frequency-doubled, 532-nm 100-ps-duration pulses with energy of ~80 mJ/pulse. Both lasers produce nearly transform-limited pulses with a beam quality $M^2 < 2$. Both laser-beam diameters were conditioned to ~8 mm using telescopes. The laser beam was passed through a coupling lens with focal length of f = +800 mm into the fiber. The hollow-core fiber (HCF) was placed in a six-axis kinematic mount, which was attached to a 1-D translational stage that moved along the laser-beam-propagation direction. This 1-m-long, 1-mm-core HCF, made by Opto-Knowledge Systems Inc., consists of capillary tubing coated with a metallic film and dielectric layer, which enables transmission of visible–infrared-wavelength light [33]. The hollow core of the HCF laser-beam delivery system was maintained at low vacuum to avoid optical breakdown at the fiber entrance or inside the fiber. The output laser beam was collimated by an f = +100-mm spherical lens and then focused at the center of the jet tube (diameter of 6.5 mm) using an achromatic spherical lens with a focal length of f=+50 mm. The beam waist at the focal point was measured by a beam profiler to be ~200 μm. A high-speed camera (Photron, SA-Z) coupled with an external two-stage intensifier [LaVision, HS-IRO (photocathode S25)] was used to track the long-lived fluorescence from the first positive band of N_2 ($B^3\Pi_g \rightarrow A\,^3\Sigma_u^+$). The emission was collected with a Nikon 50-mm $f/1.8$ lens at a wavelength range of 550–700 nm through a bandpass filter. The camera was operated at 200 kHz to track the fluorescence signal displacement for determination of flow velocities.

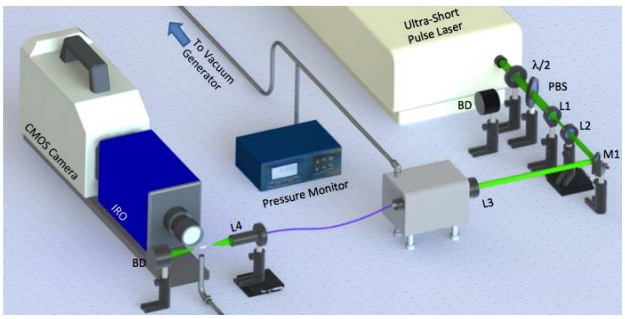

Fig. 1. Schematic diagram of fiber-coupled, ultrashort-pulse-laser-based, electronic-excitation tagging-velocimetry system. λ/2, half-wave plate; PBS, polarized beam splitter; BD, beam dump; L1, L3, L4, convex lenses; L2, concave lens.

3. CHARACTERIZATION OF HCF FOR PLEET AND FLEET

The design and performance of an ideal fiber-optic beam-delivery system for PLEET and FLEET velocimetry applications are based on three crucial parameters: 1) delivery of the required high-energy/intensity laser pulses, 2) retention of the spectral and temporal bandwidth of the input pulse during propagation through the fiber, and 3) delivery of a high-quality laser beam. Therefore, the objective of this fiber study is focused on these three aspects of ps and fs pulses propagation through the HCF.

3.1 Damage threshold

The major obstacles to fiber delivery of very high-energy/intensity laser pulses arise from optical breakdown at the entrance of the fiber and/or inside the fiber. Additionally, high-intensity beams can interact

with the medium (e.g., air) in the hollow-core fiber and cause spectral broadening of the laser beam through self-phase modulation. To solve these two problems, the hollow-core fiber-delivery system was operated in low-pressure conditions (~0.1 bar). Figure 2 shows that the 1-m-long HCF can transmit ~45 mJ/pulse and ~2.9 mJ/pulse for a 100-ps pulse and a 100-fs pulse, respectively. Such energy exceeds the required pulse energy for PLEET and FLEET applications. Because of the large core size of the fiber, the HCF is capable of coupling the maximum-pulse-energy output from the ps and fs lasers (10-Hz ps laser ~75 mJ/pulse; 1-kHz fs laser ~4.8 mJ/pulse). For the 532-nm ps laser and the 810-nm fs laser, the maximum fiber-transmission efficiency reaches ~60% at a pressure of 0.1 bar. The transmission efficiency for both cases decreases with an increase in gas pressure inside the fiber. Clearly, lower pressure (i.e., lower air density) can reduce the optical breakdown, and hence prevent laser-energy absorption by the plasma. The effect of pressure on the fiber transmission of the fs pulse is relatively small compared to that in the ps-pulse case. The reduced pressure dependence in fs-laser pulse delivery may be understood as follows: when the plasma is formed by the intense and short fs pulse, a significant portion of the pulse has already passed through the plasma (plasma-formation time ~tens of fs); thus, only the tail end of the pulse can be absorbed by the plasma. Also, because of the complete absence of avalanche breakdown process, fs laser produces very low plasma density. In contrast, a long ps pulse experiences greater absorption during the plasma-formation process and a higher plasma density is generated [34].

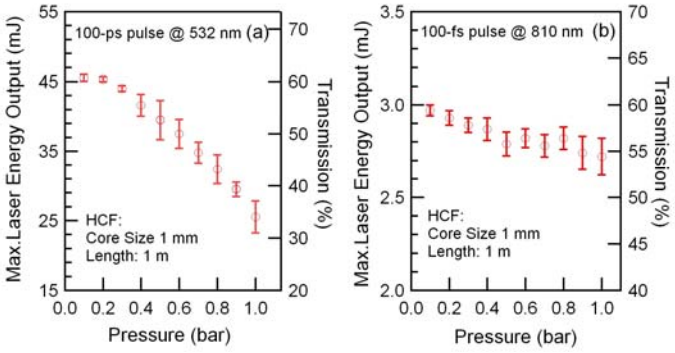

Fig. 2. Maximum output of 100-ps laser pulses at 532 nm (a) and 100-fs laser pulses at 810 nm (b) from 1-m-long HCF as a function of in-line pressure of the fiber. The input laser energies for 100-ps and 100-fs pulses are 75 mJ/pulse and 4.8 mJ/pulse, respectively.

3.2 Spectral and temporal broadening

Laser-pulse spectral broadening due to fiber propagation may reduce the efficiency of the nitrogen-dissociation process and may cause a lower nitrogen-fluorescence signal for PLEET and FLEET. Spectral broadening due to nonlinear effects in the fiber such as self-phase modulation [35] and stimulated Raman scattering [32,36] becomes noticeable with the transmission of an intense laser beam. The spectral broadening of the narrowband 100-ps pulse and broadband 100-fs pulse at incident energies of ~75 mJ and ~4.5 mJ, respectively, for an in-line gas pressure of 0.1 bar and 1 bar is shown in Fig. 3. Fiber delivery of intense ps and fs laser pulses can cause spectral broadening due to the aforementioned nonlinearities [24,25]. The observed spectral broadening for both ps and fs laser propagation is small. Lower in-line gas pressure can further reduce the spectral broadening for both cases. Here, the observed asymmetric spectral profile of the fs pulse shown in Fig. 3 could be the result of a slight misalignment of the grating-pulse compressor of the fs laser.

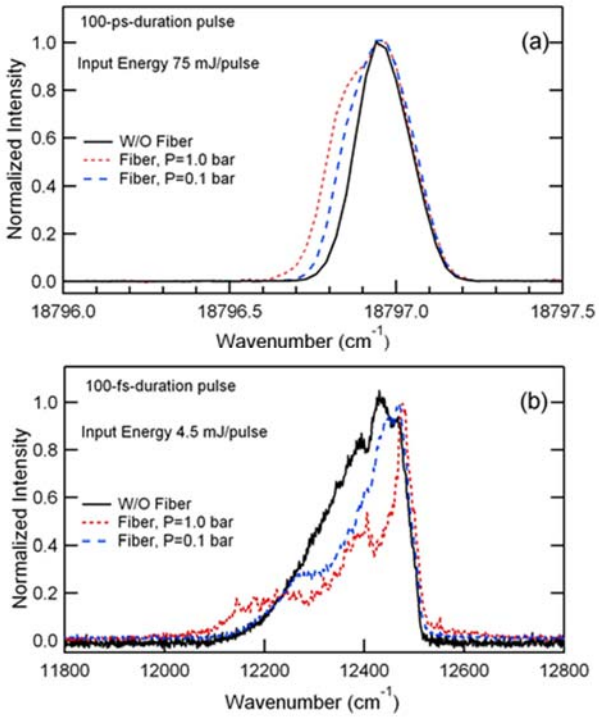

Fig. 3. Measured laser-power spectra of (a) narrowband 100-ps-duration pulse and (b) broadband 100-fs-duration pulse after 1-m-long, 1-mm-core HCF propagation under pressure of 1 bar and 0.1 bar. Original input-laser spectra are also shown (black solid line).

In addition to spectral broadening, the pulse can be broadened temporally during its propagation through the fiber because of dispersion within the fiber. The temporal broadening for a 100-fs-duration laser pulse with energy of ~1 mJ/pulse transmitting through an air-filled HCF has been investigated by Li et al. [32]. Their studies have shown that the temporal broadening of the output pulse at the fiber exit is small (<10%). We conducted temporal pulse-width measurements for a 100-ps pulse propagating through the 1-m-long HCF with a 25-GHz photodiode (Newport Model 1414) and a 20-GHz oscilloscope (Agilent Technologies DSO-X 92004A). The measured pulse width at the fiber exit was found to be nearly the same as the input laser pulse.

3.3 Output laser-beam quality

The spatial resolution of ultrashort-pulse, laser-based, electronic-excitation tagging velocimetry is determined by the beam quality of the input laser pulse at the probe volume. Figure 4 displays the output-beam profiles of the ps laser and the fs laser from the 1-m-long and 1-mm-core HCF. The intensity distribution exhibits random variation in some areas that may appear as speckles. The speckle pattern results from the interference between the many guiding modes, each travelling a slightly different path length within the fiber [37]. If the speckle pattern has a low spatial frequency (i.e., large bright and dark areas adjacent to each other), then in some areas at a focal point, sufficient N_2 fluorescence might not be generated for flow-velocity tracking. Noted that the speckle patterns vary with the input beam profile as well as fiber bending conditions.

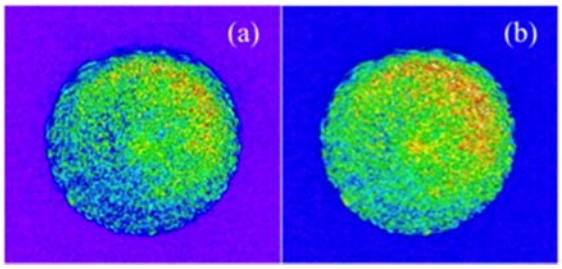

Fig. 4. False-color image of output from 1-m-long 1-mm-core HCF. Output-beam profiles of (a) ps-laser beam (532 nm) and (b) fs-laser beam (810 nm).

The focusing ability of the laser beam is determined by the beam-quality factor M^2, which is a crucial for determining the spatial resolution of fiber-coupled, electronic-excitation tagging velocimetry. Moreover, because generation of the N_2 fluorescence signal is proportional to the intensity of the excitation-laser beam, the signal generation is, in principle, strongly determined by the ability to focus the laser beam, i.e., M^2. The best possible beam quality is achieved for a diffraction-limited Gaussian beam where $M^2 = 1$ [38]. The M^2 value will increase as the beam-focusing ability decreases. The M^2 measurement method is described in Refs. [24,25]. The measured M^2 and output divergence half angle of the HCF is shown in Table 1. Because of the large M^2 value, short focal-length lens is required for fiber-coupled PLEET and FLEET measurements, limiting the working distance.

Table 1. Divergence angle and beam quality M^2

Internal Diameter	Laser Wavelength	Output Divergence Half Angle	M^2
1.0 mm (Straight fiber)	532 nm	~0.06 rad	~140
1.0 mm (Straight fiber)	810 nm	~0.06 rad	~120

4. FIBER-COUPLED PLEET AND FLEET

A proof-of-principle demonstration of velocimetry measurements using fiber-coupled PLEET and FLEET was conducted in a free jet (diameter of 6.5 mm) of nitrogen. The pulse energy used for fiber-coupled PLEET and FLEET was ~40 mJ/pulse (100-ps-duration pulse) and ~2.3 mJ/pulse (100-fs-duration pulse), respectively. Figures 5(a) and 5(b) show single-shot fiber-coupled PLEET and FLEET velocimetry-image sequences of the free N_2 jet, respectively. For both measurements, the laser beam passes through the flow at ~4 mm above the jet exit, which is about Y/D = 0.6. The jet exit is at the bottom of the images, and nitrogen gas is flowing upward. Note that the flow speeds are different for the FLEET and PLEET experiments. Measurements were conducted at 200 kHz, i. e., 5 μs between two consecutive images. The camera intensifier gate was 200 ns with 70% gain. For both cases, the starting points were 2 μs after the laser excitation. The shape of the nitrogen-fluorescence signal shown in Fig. 5 is typically a point rather than a line because a short focal-length lens was used. The point-like signal size is advantageous for two-component velocity measurements [19]. By measuring the displacement along the Y and X directions between two consecutive images, two-component velocity (i.e, V_y and V_x) can be calculated. If a second camera view is added, a third velocity component can be measured [21].

Figure 5 shows that both PLEET and FLEET signals are moving with the flow. At the early time delay (t=5 μs), the signal-to-noise ratio (SNR) is ~ 30:1 and ~ 15:1 for fiber-coupled PLEET and fiber-coupled FLEET, respectively. The size of the PLEET emission shown in Fig. 5(a) becomes larger at a longer delay time because of turbulence and diffusion. The spot size of FLEET-signal also becomes larger at the downstream of the flow. However, because of the relatively short lifetime compared to PLEET, the FLEET signals appear to be weaker at longer decay times [19,20]. As a result, the size of the FLEET signal shown in Fig. 5(b) appears to be smaller for the longer delay time.

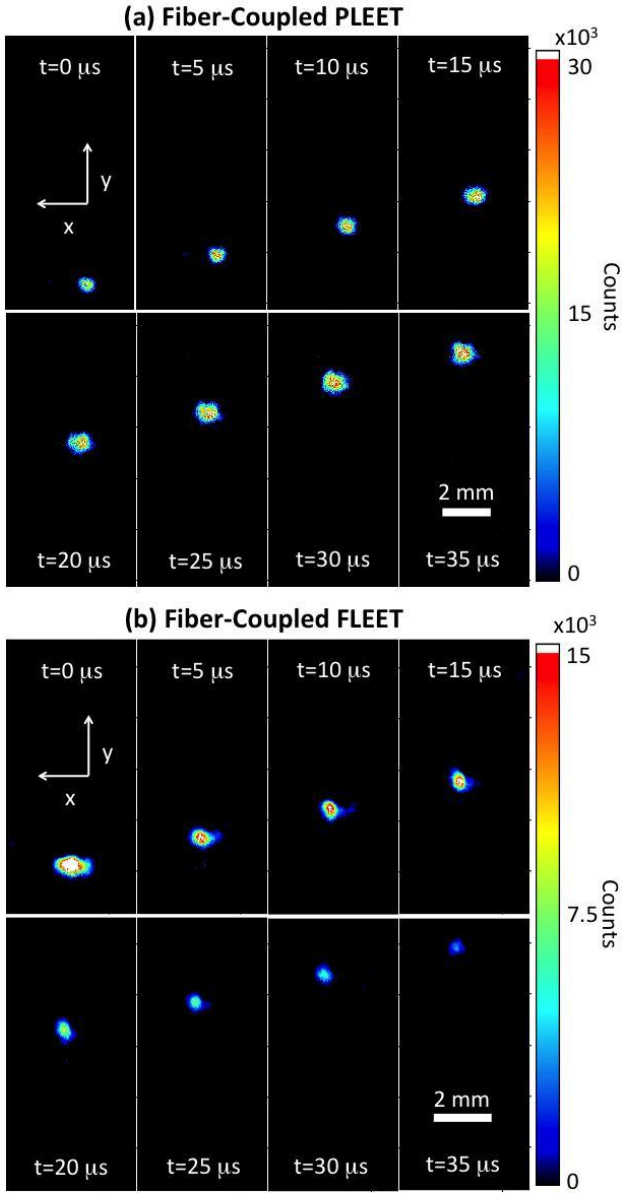

Fig. 5. (a) PLEET and (b) FLEET images with fiber-coupled beam delivery. Camera recorded images at 200-kHz rate.

Analysis of the velocity measurements for the two jet flows employing fiber-coupled PLEET and FLEET is shown in Fig. 6, which is based on the PLEET and FLEET images shown in Fig. 5. For each point, the accurate determination of the center of the PLEET and FLEET signal was analyzed by the center-mass method with Matlab [19]. Both V_y and V_x velocities were obtained using this method. For both cases the

measured V_y velocity, which is along the flow direction, remains almost constant for a certain distance and then decreases with longer time delay (i. e., away from the jet exit). Additionally, the measured speed V_x varies significantly at a longer time delay, which could result from the natural flow turbulence behavior or large uncertainties associated with relatively poor SNR.

The working distance of the current flow velocity measurement system is limited by the parameters associated with HCF delivery. Although the low-vacuum HCF delivery does not cause significant temporal and spectral broadening of the output ps and fs pulses, poor beam quality at the output of the fiber degrades the PLEET and FLEET signal level and limits the working distance. This could be improved by using a specially designed air-guided, hollow-core, photonic crystal fibers (HC-PCFs) [39,,40], which may make it possible to deliver laser pulses of sufficient energy with higher beam quality to achieve ideal fiber-coupled PLEET and FLEET measurements.

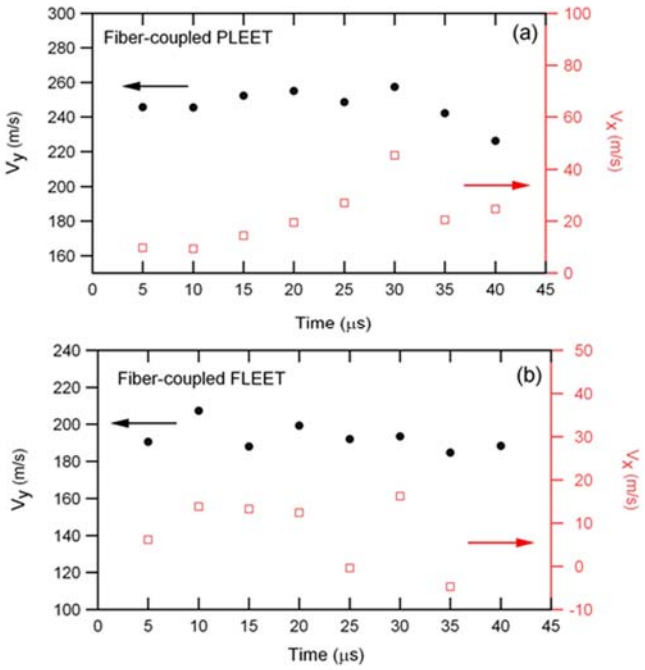

Fig. 6. Measured velocity along x- axis and y-axis from Fig. 5.

5. SUMMARY

The feasibility of delivering intense ultrashort ps and fs laser pulses through optical fibers for electronic-excitation tagging velocimetry was investigated. It was demonstrated that the propagation of ps and fs laser pulses through HCFs allows transmission of sufficient laser energy for performing PLEET and FLEET velocimetry in atmospheric-pressure N_2 jet flows. It was also determined experimentally that maintaining low-pressure at the core of the HCF beam-delivery system can reduce the probability of optical breakdown at the entrance of the fiber and/or inside the fiber and, hence, not only prevent fiber damages but also improve fiber transmissions. Additionally, this beam-delivery system also reduces spectral broadening of the input laser beam, which could lead to efficient nitrogen dissociation and achieve high PLEET and FLEET signals.

Proof-of-principle, single-laser-shot, fiber-coupled, ps- and fs-laser, electronic-excitation tagging velocimetry in a nitrogen jet was demonstrated. These results hold promise for extending the application of fiber-coupled PLEET and FLEET measurements to harsh and physically restricted environments in large ground-test facilities.

Funding Information. NASA SBIR (NNX15CL24C); Air Force Office of Scientific Research (15RQCOR202, 14RQ06COR)

Acknowledgments. The authors thank Mr. Ethan Legge for his help in laser alignment and building the vacuum device. This document has been approved for public release by AFRL (Distribution A, No. 88ABW-2017-4821) and NASA (xxxxx).

REFERENCES

1. R. J. Andrian, "Twenty years of particle image velocimetry," Exp. Fluids **39**, 159–169 (2005).
2. J. Westerweel, G. E. Elsinga, and R. J. Adrian, "Particle image velocimetry for complex and turbulent flows," Ann. Rev. Fluid Mech. **45**, 409–436 (2013).
3. B. Hiller, R. A. Booman, C. Hassa, R. K. Hanson "Velocity visualization in gas flows using laser-induced phosphorescence of biacetyl," Rev. Sci. Instrum. **55**, 1964–1967 (1984).
4. W. R. Lempert, N. Jiang, S. Sethuram, and M. Samimy, "Molecular tagging velocimetry measurements in supersonic microjets," AIAA J. **40**, 1065–1070 (2002).
5. W. R. Lempert, M. Boehm, N. Jiang, S. Gimelsein, and D. Levin, "Comparison of molecular tagging velocimetry data and direct simulation Monte Carlo simulations in supersonic micro jet flows," Exp. Fluids **34**, 403–411 (2003).
6. R. L. McKenzie, "Measurement capabilities of planar Doppler velocimetry using pulsed lasers," Appl. Opt. **35**, 948–964 (1996).
7. B. S. Thurow, N. Jiang, J. H. Kim, W. R. Lempert, and M. Samimy, "Issues with measurements of the convective velocity of large-scale structures in the compressible shear layer of a free jet," Phys. Fluids **20**, 066101 (2008).
8. J. W. Foreman Jr., E. W. George, and R. D. Lewis, "Measurement of localized flow velocities in gases with a laser Doppler flowmeter," Appl. Phys. Lett. **7**, 77–78 (1965).
9. Q. Wang, K. D. Squires, and L. P. Wang, "On the effect of non-uniform seeding on particle dispersion in two-dimensional mixing layers," Phys. Fluids **10,** 1700–1714 (1998)**.**
10. D. P. Hart, "PIV error correction," Exp. Fluids **29**, 13–22 (2000).
11. R. B. Miles, C. Cohen, P. Howard, S. Huang, E. Markovitz, and G. Russell, "Velocity measurements by vibrational tagging and fluorescent probing of oxygen," Opt. Lett. **12**, 861 (1987).
12. R. B. Miles, J. Grinstead, R. H. Kohl, and G. Diskin, " The RELIEF flow tagging technique and its application in engine testing facilities and for helium-air mixing studies," Meas. Sci. Technol. **11**, 1272-1281 (2000).
13. W.R. Lempert, Y. Zuzeek, M. Uddi, K. Frederickson, N. Jiang, S. Roy, T. Meyer, S. Gogineni, and J.R. Gord, "RELIEF velocimetry using picosecond tagging and Nd:YAG-based interrogation," AIAA-**2006-2970** (2006).
14. J.N. Forkey, N. D. Finkelstein, W. R. Lempert, and R. B. Miles, "Demonstration and characterization of filtered Rayleigh scattering for planar velocity measurements," AIAA journal, **34**, 442–448, (1996).
15. R. G. Seasholtz, A. E. Buggele, and M. F. Reeder, "Flow measurements based on Rayleigh scattering and Fabry-Perot interferometer." Opt. Lasers Eng. **27**, 543-570 (1997)
16. A. F. Fagan, M. M. Clem, and K. A. Elam, "Improvement in Rayleigh scattering measurement accuracy," AIAA-2012-1060 (2012).
17. E.B. Cummings, "Laser-induced thermal acoustics: simple accurate gas measurements," *Optics letters,* **19**, 1361–1363, (1994).

18. N. J. Dam, R. J. H. Klein-Douwel, N. M. Sijtsema, and J. J. ter Meulen, "Nitric oxide flow tagging in unseeded air," Optics Letters, **26**, 36–38, (2001).
19. N. Jiang, J. G. Mance, M. N. Slipchenko, J. J. Felver, H. U. Stauffer, T. Yi, P. M. Danehy, and S. Roy, "Seedless velocimetry at 100 kHz with picosecond-laser electronic-excitation tagging," Opt. Lett. **42**, 239–242 (2017).
20. J. B. Michael, M. R. Edwards, A. Dogariu, and R. B. Miles, "Femtosecond laser electronic excitation tagging for quantitative velocity imaging in air," Appl. Opt. **50**, 5158–5162 (2011).
21. P. M. Danehy, B. F. Bathel, N. D. Calvert, A. Dogariu, and R. B. Miles, "Three component velocity and acceleration measurement using FLEET," AIAA Paper 2014-2228 (2014).
22. R. Burns, P. M. Danehy, S. B. Jones, B. R. Halls, and N. Jiang, "Application of FLEET velocimetry in the NASA Langley 0,3-meter transonic cryogenic tunnel," *AIAA Paper 2015-2566,* 31st Aerodynamic Measurement Technology and Ground Testing Conference, Dallas, TX, June 22-26 (2015).
23. N. Jiang, B. R. Halls, H. U. Stauffer, P. M. Danehy, J. R. Gord, and S. Roy, "Selective two-photon absorptive resonance femtosecond-laser electronic-excitation tagging velocimetry," Opt. Lett. **41**, 2225–2228 (2016).
24. P. S. Hsu, W. D. Kulatilaka, J. R. Gord, and S. Roy, "Single-shot thermometry using fiber-based picosecond coherent anti-Stokes Raman scattering (CARS) spectroscopy," J. Raman. Spectrosc. **44**, 1330–1335 (2013).
25. P. S. Hsu, W. D. Kulatilaka, N. Jiang, J.R. Gord, and S. Roy, "Investigation of optical fibers for gas-phase, ultraviolet laser-induced fluorescence (UV-LIF) spectroscopy," Appl. Opt. **51**, 4047–4057 (2012).
26. P. S. Hsu, W. D. Kulatilaka, J. R. Gord, and S. Roy, "Investigation of optical fibers for high-repetition-rate, ultraviolet planar laser-induced fluorescence of OH," Appl. Opt. **52**, 3108–3115 (2013).
27. P. S. Hsu, N. Jaing, J. R. Gord, and S. Roy, "Fiber-coupled, 10 kHz simultaneous OH-PLIF/PIV," Opt. Lett. **38**, 130–132 (2013).
28. A. Hongo, K. Morosawa, K. Matsumoto, T. Shiota, and T. Hashimoto, "Transmission of kilowatt-class CO_2 laser light through dielectric-coated metallic hollow waveguides for material processing," Appl. Opt. **31**, 5114–5120 (1992).
29. Y. Matsuura, G. Takada, T. Yammamoto, Y. W. Shi, and M. Miyagi, "Hollow fibers for delivery of harmonic pulses of Q-switched Nd:YAG lasers," Appl. Opt. **41**, 442–445 (2002).
30. H. Jelinkova, J. Sulc, P. Cerny, Y. W. Shi, Y. Matsuura, and M. Miyagi, "High-power Nd:YAG laser picosecond pulse delivery by a polymer-coated silver hollow-glass waveguide," Opt. Lett. **24**, 957–959 (1999).
31. R. K. Nubling and J. A. Harrington, "Hollow-waveguide delivery systems for high-power, industrial CO2 lasers," Appl. Opt. **34**, 372–380 (1996).
32. C. Li, K. P. M. Rishad, P. Horak, Y. Matsuura, and D. Faccio, "Spectral broadening and temporal compression of ~ 100 fs pulses in air-filled hollow core capillary fibers," Opt. Express **22**, 1143–1151 (2014).
33. J. M. Kriesel, N. Gat, and D. Plemmons, "Fiber optics for remote delivery of high power pulsed laser beams," AIAA Paper 2010-1305, 48th AIAA Aerospace Sciences Meeting Including the New Horizons Forum and Aerospace Exposition, Orlando, FL, January 4-7 (2010).
34. A. Vogel, J. Noack, G. Huttmann, and G. Paltauf, "Femtosecond-laser-produced low-density plasma in transparent biological media: A tool for the creastion of chemical, thermal and thermometchnical effects below the optical breakdown threshold," Proc. SPIE **4633A**, 23-37 (2002).
35. R. H. Stolen and C. Lin, "Self-phase-modulation in silica optical fibers," Phys. Rev. A **17**, 1448 (1978).
36. R. Pini, R. Salimbeni, M. Matera, and C. Lin, "Wideband frequency conversion in the UV by nine orders of stimulated Raman scattering in a XeCl laser pumped multimode silica fiber," Appl. Phys. Lett. **43**, 517–518 (1983).
37. X. Zhu, A. Schulzgen, H. Li, H. Wei, J. V. Moloney, and N. Peyghambarian, "Coherent beam transformations using multimode waveguides," Opt. Express **18,** 7506–7520 (2010).
38. M. W. Sasnett and T. F. Johnston, "Beam characterization and measurement of propagation attributes," Proc. SPIE **1414**, 21–32 (1991).
39. P. Jaworski, F. Yu, R. R. Maier, W. J. Wadsworth, J. C. Knight, J. D. Shephard and D. P. Hand, "Picosecond and nanosecond pulse delivery through a hollow-core Negative Curvature Fiber for micromachining applications." Opt. Express **21**, 22742-22753 (2013).
40. C. Dumitrache, J. Rath, and A. P. Yalin, "High power spark delivery system using hollow core Kagome lattice fibers," Materials **7**, 5700-5710, (2014).